Heliyon 10 (2024) e38920

Contents lists available at ScienceDirect

Heliyon

journal homepage: www.cell.com/heliyon

Research article

Evaluation of super resolution technology for digestive endoscopic images

Jiaxi Lin [a,b,c,1], Shiqi Zhu [a,b,c,1], Xin Gao [a,b,c], Xiaolin Liu [a,b,c], Chunfang Xu [a,b], Zhonghua Xu [d,**], Jinzhou Zhu [a,b,c,*]

[a] Department of Gastroenterology, The First Affiliated Hospital of Soochow University, Suzhou, China
[b] Suzhou Clinical Center of Digestive Diseases, Suzhou, China
[c] Key Laboratory of Hepatoaplenic Surgery, Ministry of Education, The First Affiliated Hospital of Harbin Medical University, Harbin, China
[d] Department of Orthopedics, Jintan Affiliated Hospital to Jiangsu University, Changzhou, China

ARTICLE INFO

Keywords:
Endoscopy
Super resolution
Deep learning
Digestive diseases
Computer vision

ABSTRACT

Object: This study aims to evaluate the value of super resolution (SR) technology in augmenting the quality of digestive endoscopic images.
Methods: In the retrospective study, we employed two advanced SR models, *i.e.*, SwimIR and ESRGAN. Two discrete datasets were utilized, with training conducted using the dataset of the First Affiliated Hospital of Soochow University (12,212 high-resolution images) and evaluation conducted using the HyperKvasir dataset (2,566 low-resolution images). Furthermore, an assessment of the impact of enhanced low-resolution images was conducted using a 5-point Likert scale from the perspectives of endoscopists. Finally, two endoscopic image classification tasks were employed to evaluate the effect of SR technology on computer vision (CV).
Results: SwinIR demonstrated superior performance, which achieved a PSNR of 32.60, an SSIM of 0.90, and a VIF of 0.47 in test set. 90 % of endoscopists supported that SR preprocessing moderately ameliorated the readability of endoscopic images. For CV, enhanced images bolstered the performance of convolutional neural networks, whether in the classification task of Barrett's esophagus (improved F1-score: 0.04) or Mayo Endoscopy Score (improved F1-score: 0.04).
Conclusions: SR technology demonstrates the capacity to produce high-resolution endoscopic images. The approach enhanced clinical readability and CV models' performance of low-resolution endoscopic images.

1. Introduction

Since 1983, with the advent of electronic endoscopes based on charge-coupled device (CCD) technology superseding conventional flexible fibre-optical endoscopes, the resolution of endoscopy has greatly improved [1]. High-resolution electronic endoscopy has

* Corresponding author. Department of Gastroenterology, The First Affiliated Hospital of Soochow University, #188 Shizi St., Suzhou, 215000, China.
** Corresponding author. Department of Orthopedics, Jintan Affiliated Hospital of Jiangsu University, #500 Jintan Avenue, Changzhou, 213200, China.
E-mail addresses: xuzhonghua1985@163.com (Z. Xu), jzzhu@zju.edu.cn (J. Zhu).
[1] Jiaxi Lin and Shiqi Zhu contributed equally.

https://doi.org/10.1016/j.heliyon.2024.e38920
Received 17 March 2024; Received in revised form 25 September 2024; Accepted 2 October 2024
Available online 3 October 2024

facilitated a clearer visualization of gastrointestinal lesion images for endoscopists, thereby augmenting the efficacy of disease diagnosis and treatment. Evidence from a randomized controlled trial has demonstrated the value of high-resolution endoscopes in diagnostic procedures for colorectal neoplasia [2]. Additionally, a previous study concluded that the enhancement of endoscopic resolution increased the detection rate of colon polyps by 3.8 % [3]. Currently, a limited number of electronic endoscopes employ high-definition (HD, mainly 1920 × 1080 pixels) resolution (Fuji ELUXEO VP-7000, Olympus CV-1500, and *etc.*), while a substantial proportion of endoscopes still utilize standard-definition (SD, for example 720 × 480 pixels) resolution, particularly in economically disadvantaged regions [4]. The considerable hardware costs associated with high-resolution electronic endoscopy hinder its widespread adoption.

Nowadays, for the widespread use of artificial intelligence (AI) and deep learning in the field of endoscopy, such as cancer diagnosis and polyp detection, a vast amount of endoscopic images are required as training samples for AI algorithms[5–8]. A recent study indicated that the use of low-resolution endoscopic images as training samples considerably diminishes the performance of AI algorithms [9]. Notwithstanding, there is a dearth of publicly available large databases containing HD endoscopic images for algorithm development [10]. Consequently, there is an evident need for methods capable of generating high-resolution endoscopic images from low-resolution counterparts without necessitating hardware upgrades.

Super resolution (SR) models, which are designed to generate high-resolution images from lower-resolution imaging systems, offer potential solutions for enhancing the resolution of endoscopic images. Such SR models are commonly based on three methods: reconstruction, interpolation and learning [11]. Currently, learning-based SR models, particularly those utilizing deep learning, are the most prevalently used due to their superior performance when compared to the other techniques [12]. Two widely used deep learning-based SR architectures, Swin Image Resolution (SwinIR) and Enhanced Super-Resolution Generative Adversarial Networks (ESRGAN), have played significant roles in the medical image processing field. Previous research has shown that SwinIR can significantly enhance the quality of dental panoramic radiographs and improve the detection of microaneurysms [13,14]. Similarly, the group led by Jianshe Shi found that ESRGAN can improve the reconstruction of pneumocystis carinii pneumonia images, making the texture details of the reconstructed images clearer and the brightness information more accurate [15]. However, there is a notable dearth of research concerning the implementation of these deep learning-based SR structures in the context of endoscopic images.

In this study, we trained aforementioned two advanced deep learning-based SR models for digestive endoscopic images and evaluated their applicability from multiple perspectives, including SR metrics, endoscopist evaluation, and computer vision (CV) tasks.

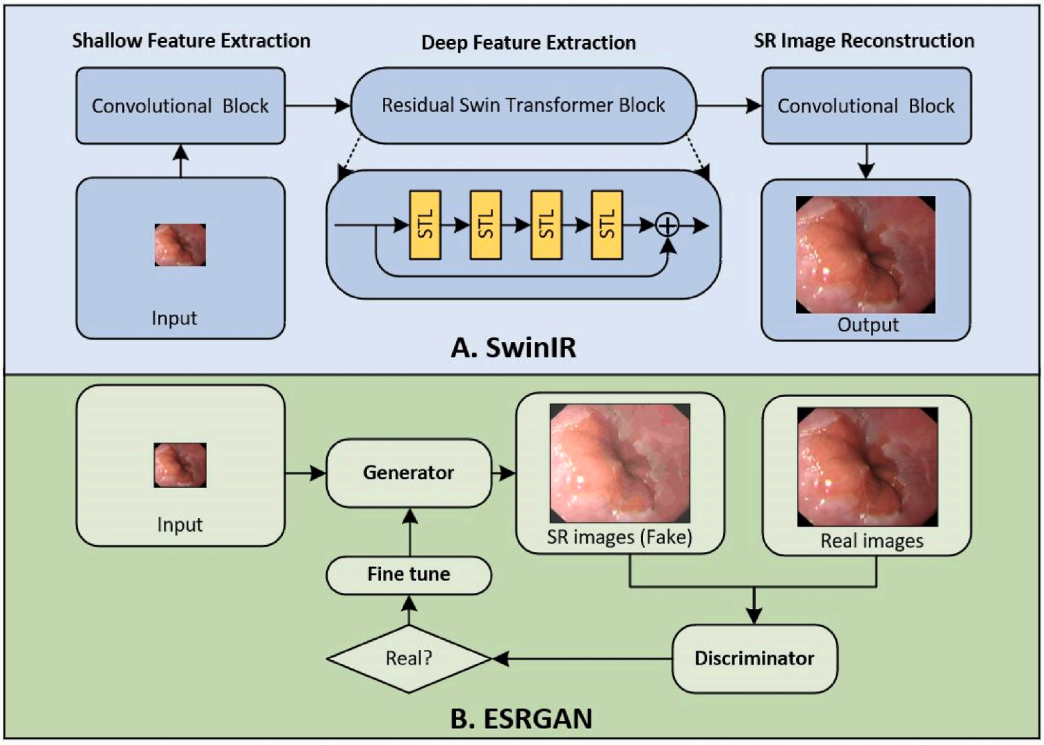

Fig. 1. The framework of super resolution models. The bule part illustrated the structures of SwinIR, while the green part illustrated the structures of ESRGAN. Three main components (shallow feature extraction, deep feature extraction, and SR image reconstruction) constituted SwinIR. Two components (generator and discriminator) constituted ESRGAN. STL: Swim transformer layers.

2. Materials and methods

2.1. Endoscopic image datasets

In this retrospective study, the raw endoscopic images were extracted independently from the following two datasets: 1) Soochow dataset. The Soochow dataset was derived from the digestive endoscopy centre, The First Affiliated Hospital of Soochow University, one of the largest endoscopy centers on China's east coast. The endoscopic imaging system in the centre was Fuji ELUXEO VP-7000, which could natively provide high-resolution (1920 × 1080 pixels) images. The Soochow dataset was incorporated by images taken from high-resolution videos of upper- and lower-gastrointestinal endoscopic examination or treatment. 2) HyperKvasir dataset. The HyperKvasir dataset is a comprehensive multiclass image and video dataset for gastrointestinal endoscopy developed by Bærum Hospital in Norway [16]. The image and video data in the dataset were collected using standard endoscopy equipment from Olympus (Olympus Europe, Germany) and Pentax (Pentax Medical Europe, Germany). We extracted the labelled images of the upper and lower gastrointestinal tract from the HyperKvasir dataset. The resolution of endoscopic images varies from 352 × 332 pixels to 989 × 873 pixels.

In this study, the Soochow dataset served as the training data, whereas the HyperKvasir dataset was employed for test purposes. Datasets used for training and testing are mutually exclusive.

2.2. Endoscopic image preprocessing

Endoscopic images were initially subjected to a manual review process. All endoscopic images derived from the previously mentioned datasets were meticulously reviewed by two senior endoscopists. The endoscopic images that were severely blurred, out of focus or subject to significant lighting changes due to violent camera movements were systematically excluded. To generate the low-resolution images required for training, the reviewed endoscopic images were downsampled using 4X (i.e., quadruple magnification) bicubic interpolation. All images were standardized to the JPG format.

2.3. SR model development

Two SR models, Swin Image Resolution (SwinIR) and Enhanced Super-Resolution Generative Adversarial Networks (ESRGAN) based on different structures, were trained. The framework illustrating the two SR models is shown in Fig. 1. The scale factors for both models were 4X.

SwinIR: SwinIR, proposed by ETH Zurich in 2021, marked a significant achievement in the application of transformer structures within the realm of image restoration [17]. The novelty of SwinIR is its incorporation of the Swin transformer [18]. During the training procedure, we employed the transfer learning approach, which could facilitate the utilization of prior knowledge. Different configurations were used for the image reconstruction module of SwinIR when training. Three distinct sets of pretrained weights (classical weight, lightweight weight and real-world weight) were applied. Concurrently, a variety of upsampling methods, such as pixelshuffle and nearest + conv, were adopted to explore the potential impact of different upsampling methods on model performance. Table S1 shows the details of the pretrained weights and upsampling methods.

ESRGAN: ESRGAN is relevant in the application of generative adversarial networks (GANs) within the domain of image restoration [19]. ESRGAN comprises two primary components: a generator and a discriminator. The objective of the generator was to deceive the discriminator by fabricating images that appear authentic, whereas the discriminator's role was to differentiate between these artificially produced images and real ones.

2.4. SR models' evaluation

To conduct a comprehensive evaluation of SR models' performance, we approached the assessment from three dimensions: objective metrics, endoscopists' perspectives and CV tasks.

1. **Objective metrics:** We utilized three widely accepted metrics for SR model evaluation: peak signal-to-noise ratio (PSNR), structure similarity index measure (SSIM), and visual information fidelity (VIF). The details of these metrics are summarized in Table S2.
2. **Endoscopists' perspective:** The perspectives of endoscopists observing SR endoscopic images were utilized to assess the clinical applicability of the models. Unprocessed, low-resolution images of three typical lesions, including ulcers, polyps, and early cancer, were extracted from the Soochow dataset and HyperKvasir dataset, with each lesion represented by a set of 10 images. All images were SR processed before being compared. A total of 10 endoscopists (4 senior and 6 junior endoscopists) were incorporated into the evaluation phase. Their perspectives were quantitatively assessed using a 5-point Likert scale, a well-established tool for gauging opinions [20]. The scale was structured to encapsulate five levels of agreement: 'Strongly disagree' (1 point), 'Disagree' (2 points), 'Neutral' (3 points), 'Agree' (4 points), and 'Strongly agree' (5 points). The details of the Likert scales are provided in Table S3. The cronbach's alpha is calculated to assess the reliability of each item in the Likert scales.
3. **Computer vision tasks:** The influence of endoscopic images after SR processing on CV was assessed. Two CV classification tasks pertaining to the upper- and lower-gastrointestinal tract (namely, Barrett's esophagus classification task and Mayo Endoscopy Score (MES) for Ulcerative colitis classification task) were employed [21]. Detailed descriptions of these two tasks are provided in Table S4. Two classical CNN structures (DenseNet121 and DenseNet169), with DenseNet as the backbone, were utilized for the CV

tasks [22]. Data from both tasks were randomly partitioned into a CV-training set and a CV-validation set at a ratio of 8:2 for model development and performance comparison. The data in the CV-validation set were not enhanced to ensure fairness of the comparison. The flowchart of the two tasks is shown in Fig. 2. Evaluation indicators included F1-score, accuracy, precision, and recall.

3. Results

3.1. Endoscopic image datasets

A total of 12,212 endoscopic images, comprising 5,762 upper gastrointestinal images and 6,450 lower gastrointestinal images, were extracted from the endoscopy videos of 17 patients in the Soochow dataset to form the training set. Conversely, 2,566 images, including 1,455 upper gastrointestinal images and 1,111 lower gastrointestinal images, were extracted from the HyperKvasir dataset to serve as the testing set. The details of the incorporated endoscopic images in the training set are presented in Table S5.

4. SR metrics

Table 1 presents the performance of SR models. Within the training set, the SwinIR model, utilizing the 'classical pretrained weight' and 'pixelshuffle sampling method', demonstrated superior performance compared to other models, as evidenced by the following SR metrics: PSNR (36.84), SSIM (0.97), and VIF (0.69). Similarly, in the test set, the SwinIR model continued to outperform other models, achieving notable SR metrics: PSNR (32.60), SSIM (0.90), and VIF (0.47). Subsequent model evaluations are based on this model, which exhibits optimal SR metrics. The comparison between SR images and original images is shown in Fig. 3.

4.1. Endoscopists' evaluation

The primary endoscopists' opinions are summarized in Table S6. The visualization of the 5-point Likert scale of endoscopists is illustrated in Fig. 4. A substantial majority, 90 %, of the endoscopists affirmed the efficacy of SR technology in augmenting the clarity of endoscopic images and enhancing diagnostic precision. When evaluating three distinct disease types, 90 % of endoscopists concurred that SR technology noticeably improved the visibility of polyps. Conversely, the technology's effectiveness in enhancing the image quality of early-stage cancer was endorsed by a significantly smaller fraction of endoscopists, standing at 40 %. Cronbach's alpha for each item is summarized in Table S7, which demonstrates that most of the items have acceptable reliability.

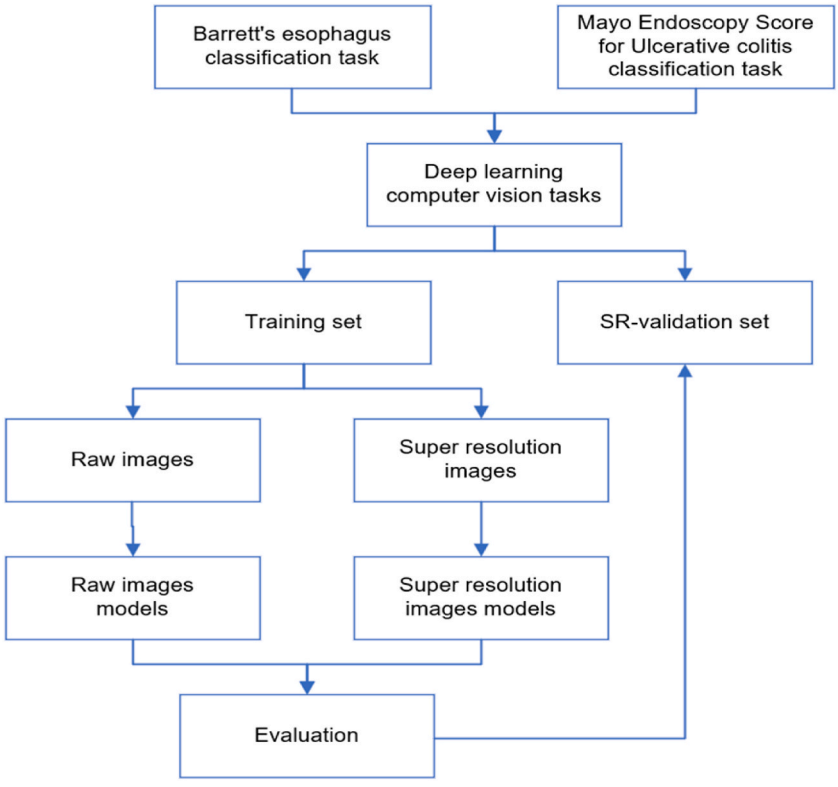

Fig. 2. The flowchart of two deep learning computer vision tasks.

Table 1
The performance of super resolution models in the training and test sets.

Model	Pre-trained weight	Sampling method	Training set			Test set		
			PSNR	SSIM	VIF	PSNR	SSIM	VIF
SwinIR	Realworld	nearest + conv	32.87	0.93	0.55	29.76	0.82	0.41
SwinIR	Realworld	pixelshuffle	35.90	0.97	0.68	32.44	0.89	0.45
SwinIR	lightweight	pixelshuffle	35.68	0.97	0.68	32.43	0.89	0.45
SwinIR	classical	nearest + conv	36.28	0.97	0.69	32.46	0.89	0.45
SwinIR	classical	pixelshuffle	**36.84**	**0.97**	**0.69**	**32.60**	**0.90**	**0.47**
ESRGAN	SRx4_official	–	36.55	0.96	0.61	31.29	0.85	0.39

Footnotes: PSNR: peak signal-to-noise ratio. SSIM: structure similarity index measure. VIF: visual information fidelity.

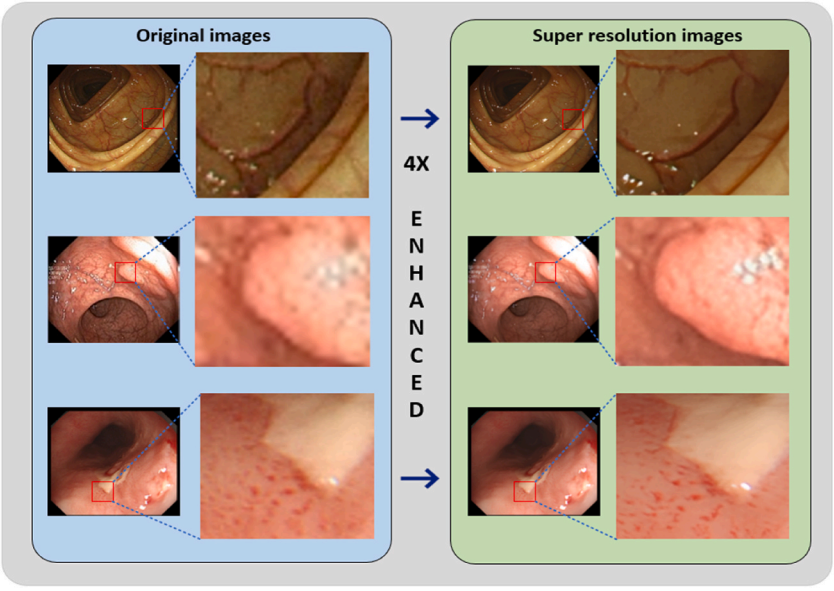

Fig. 3. Comparison between super resolution images and original images.

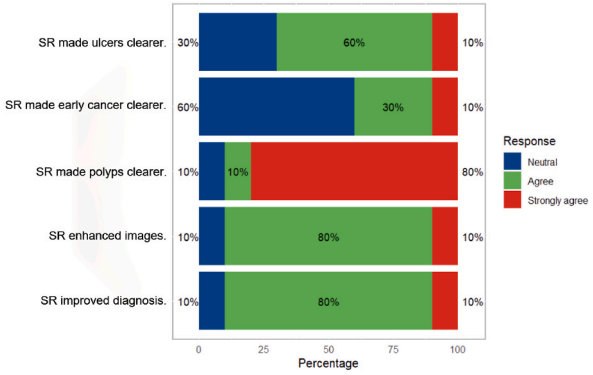

Fig. 4. Visualization of the 5-point Likert scale of endoscopists. SR: Super resolution.

4.2. Computer vision tasks

Table 2 shows the results of two CV tasks in the CV-validation. The endoscopic images after 4X SR improve the performance of both models. For the classification task of Barrett's esophagus, DenseNet121 with SR images outperformed with metrics: F1-score (0.85), accuracy (0.86), precision (0.89), and recall (0.82). For the Mayo endoscopy score classification task, DenseNet169 with SR images showed superior performance compared to the other models.

Table 2
The performance of convolutional neural networks with super resolution endoscopic images in the CV-validation set.

Model	Dataset	F1-score	Accuracy	Precision	Recall
Densenet121	Barrett-LR	0.81	0.81	0.80	0.81
	Barrett-HR	**0.85**	**0.86**	**0.89**	**0.82**
	Mayo-LR	0.72	0.73	0.73	0.72
	Mayo-HR	**0.76**	**0.76**	**0.79**	**0.75**
Densenet169	Barrett-LR	0.82	0.82	0.84	0.80
	Barrett-HR	**0.84**	**0.85**	**0.89**	**0.80**
	Mayo-LR	0.73	0.75	0.75	0.73
	Mayo-HR	**0.77**	**0.76**	**0.77**	**0.76**

Footnotes: Barrett-LR: The Barrett's esophagus dataset included low-resolution images. Barrett-HR: The Barrett's esophagus dataset included high-resolution images. Mayo-LR: The Mayo Endoscopy Score dataset included low-resolution images. Mayo-HR: The Mayo Endoscopy Score dataset included high-resolution images.

5. Discussion

In this study, we evaluated the application of SR approach in digestive endoscopic images. Two advanced SR models were developed, and SR technology was thoroughly evaluated from the perspectives of clinical value and potential application in CV. Our findings support that SR enhances the endoscopist's experience of interpreting endoscopic images and can improve diagnostic accuracy to a certain degree. Moreover, it demonstrated that the performance of CV models could be enhanced by employing SR without the need to increase the training sample size.

The concept of SR was initially proposed by Gerchberg [23] to interpret the enhancement of an optical system's resolution beyond the diffraction limit. Over recent years, this concept has evolved into a method capable of generating high-resolution images from low-resolution counterparts. SR has been applied in various fields, including computer graphics, surveillance, and, notably, medical images[24–26]. Several studies have explored the impact of SR technology on computed tomography (CT) and magnetic resonance imaging, including improving the temporal resolution of cine cardiac MRI sequences, augmenting low-dose 18F-FDG PET data, and improving the accuracy of CT tumour staging[27–29]. However, in the realm of endoscopic imagery, a review of previous studies reveals a dearth of related research and a lack of clinician involvement. For instance, Chen W et al. [30]proposed a dynamic depth-aware network for endoscopy SR using the Kvasir dataset and the EndoScene dataset, while Lin J et al. [31]developed a quaternion attention multiscale widening network for SR endoscopic image using the CVC ClinicDB and Kvasir datasets. In comparison to these studies, our model demonstrated superior SR metrics when adopting the same scale factors (4X). The PSNR in our model was 36.84, which was higher than that of Lin J's model (34.50). This improved performance may be attributed to our utilization of a self-constructed large sample HD dataset and the application of the state-of-the-art SR model based on the Swin transformer architecture. Furthermore, our study incorporated evaluations from frontline clinical endoscopists to analyse the value of the SR technique in identifying tumours, ulcers, and polyps.

Prior studies have demonstrated that the resolution of training images significantly impacts the performance of AI algorithms, regardless of whether they are X-ray or endoscopic images [9,32]. Insufficient image resolution often leads to suboptimal model performance. Previous studies have ascertained that enhancing image resolution using SR technology bolsters AI-based detection and localization of colonic polyps [33]. Nonetheless, there is a paucity of research concerning endoscopic image classification tasks. In our investigation, we focused on two tasks: the classification of Barrett's esophagus and the Mayo score for ulcerative colitis. We discovered that the SR technique enhances the classification performance of CV models in both binary and multiclassification tasks. This improvement in performance may be attributed to the fact that SR not only augments image resolution but also incorporates external data for reconstruction, yielding images with superior detail. Consequently, our study substantiates the potential of SR technology as an efficacious image preprocessing method for endoscopic AI algorithms.

Clinically, SR technology marginally enhances the readability of endoscopic images. Our study revealed that endoscopists found SR to be most effective for bulging lesions (polyps) and to be less effective for flat lesions (early cancer). This distinction may be a consequence of the inherent SR technology characteristic that accentuates high-frequency detail, enabling the efficient differentiation of bulging polyps from the surrounding mucosa [34]. However, SR is less adept at highlighting low-frequency details, such as mucous membranes where early cancers closely resemble normal tissue under white light endoscopy.

Despite our study showing the potential clinical value and applicability of CV using SR models, it also has several limitations. First, the retrospective nature of the study leads to potential selection bias. More external test sets based on a prospective design are necessary to further verify the generalization capabilities of the model. Implementing standardized data collection protocols will help minimize selection bias and ensure consistency across participating centers. Second, the assessment of the clinical application of the SR model encompassed a limited number of diseases. As such, a more comprehensive evaluation is warranted in future research. Finally, our SR models were designed for white-light endoscopic images, leaving a gap regarding the potential use of SR technology for other endoscopy modalities, such as narrow band imaging and flexible spectral imaging colour enhancement.

6. Conclusions

In this study, we evaluated the feasibility of SR technology in the domain of digestive endoscopic imaging. We established that SR

models incorporating SwinIR possessed the capacity to drive high-resolution endoscopic images from their low-resolution counterparts. For endoscopists, SR technology could moderately ameliorate the legibility of endoscopic images and is most effective for bulging lesions. In terms of deep learning CV tasks, SR technology could improve CV models' performance by functioning as an image preprocessing approach.

Statement on consent

The ethics committee approved the consent waiver because all data is strictly de-identified. All procedures were performed strictly in accordance with the relevant guidelines and regulations, including the standards of the Declaration of Helsinki.

Ethics approval

The research was approved by the ethics committee of the First Affiliated Hospital of Soochow University (2023-055).

Data and code availability statement

The data that support the findings of this study are available from the corresponding author (Jinzhou Zhu), upon reasonable request.

CRediT authorship contribution statement

Jiaxi Lin: Writing – original draft, Formal analysis. **Shiqi Zhu:** Writing – original draft, Formal analysis. **Xin Gao:** Data curation. **Xiaolin Liu:** Data curation. **Chunfang Xu:** Writing – review & editing. **Zhonghua Xu:** Conceptualization. **Jinzhou Zhu:** Funding acquisition, Conceptualization.

Declaration of competing interest

The authors declare that they have no known competing financial interests or personal relationships that could have appeared to influence the work reported in this paper.

Acknowledgements

We would like to thank the Team AiMprism for their support during the data collection and analysis.

Funding

The work was supported by the National Natural Science Foundation of China (82000540), Suzhou Clinical Center of Digestive Diseases (Szlcyxzx202101), the Youth Program of Suzhou Health Committee (KJXW2019001), and the Open Fund of Key Laboratory of Hepatoaplenic Surgery, Ministry of Education, Harbin, China (GPKF202304).

Appendix A. Supplementary data

Supplementary data to this article can be found online at https://doi.org/10.1016/j.heliyon.2024.e38920.

References

[1] B.I. Hirschowitz, C.W. Peters, L.E. Curtiss, Preliminary report on a long fiberscope for examination of stomach and duodenum, Med. Bull. Ann Arbor Mich 23 (1957) 178–180.
[2] M. Pellisé, G. Fernández-Esparrach, A. Cárdenas, O. Sendino, E. Ricart, E. Vaquero, A.Z. Gimeno-García, C.R. de Miguel, M. Zabalza, A. Ginès, J.M. Piqué, J. Llach, A. Castells, Impact of wide-angle, high-definition endoscopy in the diagnosis of colorectal neoplasia: a randomized controlled trial, Gastroenterology 135 (2008) 1062–1068, https://doi.org/10.1053/j.gastro.2008.06.090.
[3] N.Y. Jrebi, M. Hefty, T. Jalouta, J. Ogilvie, A.T. Davis, T. Asgeirsson, M. Luchtefeld, High-definition colonoscopy increases adenoma detection rate, Surg. Endosc. 31 (2017) 78–84, https://doi.org/10.1007/s00464-016-4986-7.
[4] V. Subramanian, K. Ragunath, Advanced endoscopic imaging: a review of commercially available technologies, Clin. Gastroenterol. Hepatol. 12 (2014) 368–376.e1, https://doi.org/10.1016/j.cgh.2013.06.015.
[5] H. Luo, G. Xu, C. Li, L. He, L. Luo, Z. Wang, B. Jing, Y. Deng, Y. Jin, Y. Li, B. Li, W. Tan, C. He, S.R. Seeruttun, Q. Wu, J. Huang, D.-W. Huang, B. Chen, S.-B. Lin, Q.-M. Chen, C.-M. Yuan, H.-X. Chen, H.-Y. Pu, F. Zhou, Y. He, R.-H. Xu, Real-time artificial intelligence for detection of upper gastrointestinal cancer by endoscopy: a multicentre, case-control, diagnostic study, Lancet Oncol. 20 (2019) 1645–1654, https://doi.org/10.1016/S1470-2045(19)30637-0.
[6] G. Urban, P. Tripathi, T. Alkayali, M. Mittal, F. Jalali, W. Karnes, P. Baldi, Deep learning localizes and identifies polyps in real time with 96% accuracy in screening colonoscopy, Gastroenterology 155 (2018) 1069–1078.e8, https://doi.org/10.1053/j.gastro.2018.06.037.
[7] F. Chadebecq, L.B. Lovat, D. Stoyanov, Artificial intelligence and automation in endoscopy and surgery, Nat. Rev. Gastroenterol. Hepatol. 20 (2023) 171–182, https://doi.org/10.1038/s41575-022-00701-y.

[8] H. Chen, C. Li, X. Li, M.M. Rahaman, W. Hu, Y. Li, W. Liu, C. Sun, H. Sun, X. Huang, M. Grzegorzek, IL-MCAM: an interactive learning and multi-channel attention mechanism-based weakly supervised colorectal histopathology image classification approach, Comput. Biol. Med. 143 (2022) 105265, https://doi.org/10.1016/j.compbiomed.2022.105265.
[9] C.F. Sabottke, B.M. Spieler, The effect of image resolution on deep learning in radiography, radiol, Artif. Intell. 2 (2020) e190015, https://doi.org/10.1148/ryai.2019190015.
[10] B.B.S.L. Houwen, K.J. Nass, J.L.A. Vleugels, P. Fockens, Y. Hazewinkel, E. Dekker, Comprehensive review of publicly available colonoscopic imaging databases for artificial intelligence research: availability, accessibility, and usability, Gastrointest. Endosc. 97 (2023) 184–199.e16, https://doi.org/10.1016/j.gie.2022.08.043.
[11] K. Li, S. Yang, R. Dong, X. Wang, J. Huang, Survey of single image super-resolution reconstruction, IET Image Process. 14 (2020) 2273–2290, https://doi.org/10.1049/iet-ipr.2019.1438.
[12] S.M.A. Bashir, Y. Wang, M. Khan, Y. Niu, A comprehensive review of deep learning-based single image super-resolution. https://doi.org/10.48550/arXiv.2102.09351, 2022.
[13] B. Zhang, J. Li, Y. Bai, Q. Jiang, B. Yan, Z. Wang, An improved microaneurysm detection model based on SwinIR and YOLOv8, Bioeng. Basel Switz. 10 (2023) 1405, https://doi.org/10.3390/bioengineering10121405.
[14] H. Mohammad-Rahimi, S. Vinayahalingam, E. Mahmoudinia, P. Soltani, S.J. Bergé, J. Krois, F. Schwendicke, Super-resolution of dental panoramic radiographs using deep learning: a pilot study, Diagn. Basel Switz. 13 (2023) 996, https://doi.org/10.3390/diagnostics13050996.
[15] J. Shi, Y. Ye, H. Liu, D. Zhu, L. Su, Y. Chen, Y. Huang, J. Huang, Super-resolution reconstruction of pneumocystis carinii pneumonia images based on generative confrontation network, Comput. Methods Programs Biomed. 215 (2022) 106578, https://doi.org/10.1016/j.cmpb.2021.106578.
[16] H. Borgli, V. Thambawita, P.H. Smedsrud, S. Hicks, D. Jha, S.L. Eskeland, K.R. Randel, K. Pogorelov, M. Lux, D.T.D. Nguyen, D. Johansen, C. Griwodz, H. K. Stensland, E. Garcia-Ceja, P.T. Schmidt, H.L. Hammer, M.A. Riegler, P. Halvorsen, T. de Lange, HyperKvasir, a comprehensive multi-class image and video dataset for gastrointestinal endoscopy, Sci. Data 7 (2020) 283, https://doi.org/10.1038/s41597-020-00622-y.
[17] J. Liang, J. Cao, G. Sun, K. Zhang, L. Van Gool, R. Timofte, SwinIR: image restoration using Swin transformer. https://doi.org/10.48550/arXiv.2108.10257, 2021.
[18] Z. Liu, Y. Lin, Y. Cao, H. Hu, Y. Wei, Z. Zhang, S. Lin, B. Guo, Swin transformer: hierarchical vision transformer using shifted windows. https://doi.org/10.48550/arXiv.2103.14030, 2021.
[19] X. Wang, K. Yu, S. Wu, J. Gu, Y. Liu, C. Dong, C.C. Loy, Y. Qiao, X. Tang, ESRGAN: enhanced super-resolution generative adversarial networks. https://doi.org/10.48550/arXiv.1809.00219, 2018.
[20] R. Likert, A technique for the measurement of attitudes, Arch. Psychol. 22 140 (1932) 55.
[21] N. Mohammed Vashist, M. Samaan, M.H. Mosli, C.E. Parker, J.K. MacDonald, S.A. Nelson, G.Y. Zou, B.G. Feagan, R. Khanna, V. Jairath, Endoscopic scoring indices for evaluation of disease activity in ulcerative colitis, Cochrane Database Syst. Rev. 1 (2018) CD011450, https://doi.org/10.1002/14651858.CD011450.pub2.
[22] G. Huang, Z. Liu, L. van der Maaten, K.Q. Weinberger, Densely connected convolutional networks. https://doi.org/10.48550/arXiv.1608.06993, 2018.
[23] R.W. Gerchberg, Super-resolution through error energy reduction, Opt. Acta Int. J. Opt. 21 (1974) 709–720, https://doi.org/10.1080/713818946.
[24] X. Tao, H. Gao, R. Liao, J. Wang, J. Jia, Detail-revealing deep video super-resolution, in: 2017 IEEE Int. Conf. Comput. Vis. ICCV, 2017, pp. 4482–4490, https://doi.org/10.1109/ICCV.2017.479.
[25] D. Qiu, Y. Cheng, X. Wang, Medical image super-resolution reconstruction algorithms based on deep learning: a survey, Comput. Methods Programs Biomed. 238 (2023) 107590, https://doi.org/10.1016/j.cmpb.2023.107590.
[26] S. Lee, J.-H. Kim, J.-P. Heo, Super-resolution of license plate images via character-based perceptual loss, in: 2020 IEEE Int. Conf. Big Data Smart Comput. BigComp, 2020, pp. 560–563, https://doi.org/10.1109/BigComp48618.2020.000-1.
[27] Q. Lyu, H. Shan, Y. Xie, A.C. Kwan, Y. Otaki, K. Kuronuma, D. Li, G. Wang, Cine cardiac MRI motion artifact reduction using a recurrent neural network, IEEE Trans. Med. Imag. 40 (2021) 2170–2181, https://doi.org/10.1109/TMI.2021.3073381.
[28] Y.-R.J. Wang, P. Wang, L.C. Adams, N.D. Sheybani, L. Qu, A.H. Sarrami, A.J. Theruvath, S. Gatidis, T. Ho, Q. Zhou, A. Pribnow, A.S. Thakor, D. Rubin, H. E. Daldrup-Link, Low-count whole-body PET/MRI restoration: an evaluation of dose reduction spectrum and five state-of-the-art artificial intelligence models, Eur. J. Nucl. Med. Mol. Imag. 50 (2023) 1337–1350, https://doi.org/10.1007/s00259-022-06097-w.
[29] M. Hou, L. Zhou, J. Sun, Deep-learning-based 3D super-resolution MRI radiomics model: superior predictive performance in preoperative T-staging of rectal cancer, Eur. Radiol. 33 (2023) 1–10, https://doi.org/10.1007/s00330-022-08952-8.
[30] W. Chen, Y. Liu, J. Hu, Y. Yuan, Dynamic depth-aware network for endoscopy super-resolution, IEEE J. Biomed. Health Inform. 26 (2022) 5189–5200, https://doi.org/10.1109/JBHI.2022.3188878.
[31] J. Lin, G. Huang, J. Huang, X. Yuan, Y. Zeng, C. Shi, Quaternion attention multi-scale widening network for endoscopy image super-resolution, Phys. Med. Biol. 68 (2023), https://doi.org/10.1088/1361-6560/acc002.
[32] V. Thambawita, I. Strümke, S.A. Hicks, P. Halvorsen, S. Parasa, M.A. Riegler, Impact of image resolution on deep learning performance in endoscopy image classification: an experimental study using a large dataset of endoscopic images, Diagnostics 11 (2021) 2183, https://doi.org/10.3390/diagnostics11122183.
[33] M. Taş, B. Yılmaz, Super resolution convolutional neural network based pre-processing for automatic polyp detection in colonoscopy images, Comput. Electr. Eng. 90 (2021) 106959, https://doi.org/10.1016/j.compeleceng.2020.106959.
[34] G. Gendy, G. He, N. Sabor, Lightweight image super-resolution based on deep learning: state-of-the-art and future directions, Inf. Fusion 94 (2023) 284–310, https://doi.org/10.1016/j.inffus.2023.01.024.